

## **Thermal-Hydraulic calculations for the Westinghouse AP-1000 clean core with MITH code**

**Tariq Zakariya Malatim<sup>1</sup>, Amal S. Dakhil<sup>2</sup>**

<sup>1</sup>Libyan Atomic Energy Establishment - Energy generation technology department  
Janzour costal road 10 Km – Tripoli / Libya

[Tariqmolatim@gmail.com](mailto:Tariqmolatim@gmail.com)  
[+218-922304752](tel:+218922304752)

<sup>2</sup>University of Tripoli -Nuclear Engineering Department  
Tripoli - Libya

[Amal\\_ssd@yahoo.com](mailto:Amal_ssd@yahoo.com)

### **Abstract**

In this study, the core of the Westinghouse AP1000 reactor [1] gen. III+ was simulated, which is one of four reactors that have been nominated to be adopted by the Libyan Atomic Energy Establishment [2]. The MITH code, which is a thermal-hydraulic code, is used to find the clean core thermal parameters. The power distribution in the reactor core was evaluated using the **2DB** code [3]. The hottest assemblies, which have the maximum power production were determined with a value of 30.82 MW Using **2DB** code, the hottest assembly has been described, and the hottest channels have been found. The power produced in the hottest channel is 139 KW. Using the **MITH** code [4], the parameters of fuel elements were evaluated for average and hottest channel length, which were divided into 40 meshes for drawing and 100 meshes for studying. The temperatures of the fuel center & surface, clad, and coolant have been determined and they were satisfactory, while the minimum DNBR has been found to be within safe limits with a value of 2.17.

### **1. Introduction**

#### **1.1. AP1000 reactor core [1]**

Nuclear power plants used the Westinghouse Advanced Passive PWR AP1000, is an 1117 MWe class PWR based closely on the AP600 design. The AP1000 maintains most of the AP600 design configuration [4] and uses the AP600 components, proven in earlier Westinghouse PWRs or in special test programs, and licensing basis by limiting the changes to the AP600 design to as few as possible. In the AP1000 design, fuel rods are fabricated from cylindrical tubes made of **ZIRLO** (zirconium-based alloy(s)) containing UO<sub>2</sub> fuel pellets. Fuel assemblies are arranged in a pattern that approximates a right circular cylinder. Each fuel assembly contains a 17×17 rod array composed nominally of 264 fuel rods, 24 rod cluster control thimbles, and an in-core instrumentation thimble, which are shown in figure 1. For the initial core loading, the fuel rods within a given assembly have the same uranium enrichment. A total of 157 fuel assemblies of three different enrichments are used in the initial core loading to establish a favorable radial power distribution. Two regions consisting of the two lower enrichments, 2.35 w/o and 3.40 w/o, are interspersed to form a checkerboard pattern in the central portion of the core. The third region is arranged around the periphery of the core and contains the highest enrichment of 4.45 w/o. Figure 1 shows the core and fuel assembly of the AP1000 [5].

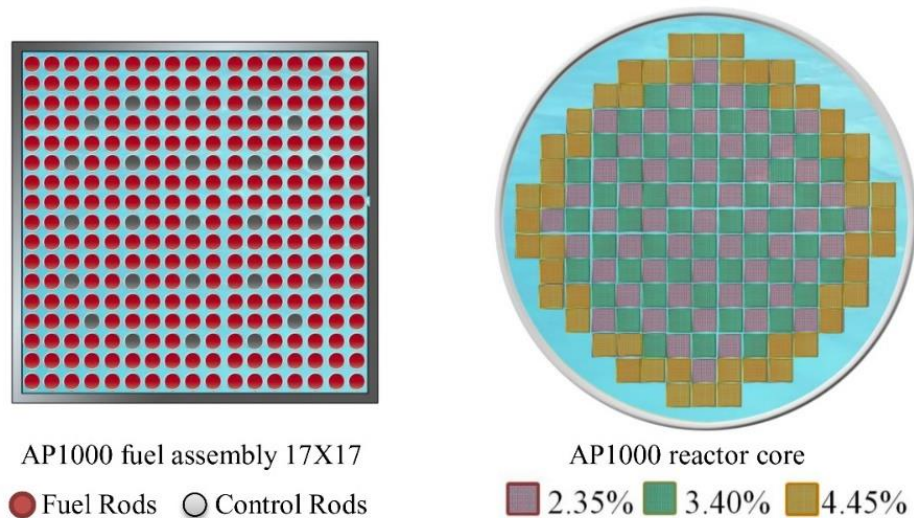


Figure 1 AP1000 reactor core & fuel assembly

### 1.2. Thermal hydraulic analysis [6]

Thermal analysis of a nuclear reactor becomes critical because it enables anchoring in practice the greatest power released in view of the reactor material properties. The maximum power generated in a reactor should be transferred from the nuclear fuel into the coolant in the form of heat. Thus, thermal analysis is a tool for validating neutronic analysis and establishing safety parameters for nuclear reactors. The maximum power to be produced by the core of a reactor is determined by the heat removal capacity in the hottest channel reactor or the fuel temperature limits in the position of the hottest point of the core. From a thermal-hydraulic standpoint, in the case of water-cooled reactors such as the AP1000, the designer's primary concern is the avoidance of critical heat flux (CHF), which is a sudden drop of the heat transfer coefficient of a surface at which coolant is evaporating or boiling. The reactors should be designed such that the fission products remain confined up to the fuel during the entire time and during adverse conditions such as normal operation, shutdown, and accident conditions when the refrigerant cannot normally cool the fuel down.

### 1.3. DNB [7]

If the heat flux of a boiling system is higher than the critical heat flux (CHF) of the system, the bulk fluid may boil, or in some cases, regions of the bulk fluid may boil where the fluid travels in small channels. Thus, large bubbles form, sometimes blocking the passage of the fluid. This results in a departure from nucleate boiling (DNB) in which steam bubbles no longer break away from the solid surface of the channel, bubbles dominate the channel or surface, and the heat flux dramatically decreases. Vapor essentially insulates the bulk liquid from the hot surface. During DNB, the surface temperature must therefore increase substantially above the bulk fluid temperature to maintain a high heat flux.

Avoiding the CHF is an engineering problem in heat transfer applications such as nuclear reactors, where fuel plates must not be allowed to overheat. DNB may be avoided in practice by increasing the pressure of the fluid, increasing its flow rate, or by utilizing a lower temperature bulk fluid that has a higher CHF. If the bulk fluid temperature is too low or the pressure of the fluid is too high, nucleate boiling is, however, not possible.

#### **1.4. MITH Code [6]**

MITH (MICHIGAN THERMAL HYDRAULIC ANALYSIS CODE) is a thermal-hydraulic analysis code that uses thermal hydraulic correlations to deal with temperature and pressure as well as power for the hot and average channel. The code calculates fuel, clad and coolant temperatures for both hot and average channel as well as core pressure drop, fluid density and fluid quality, and it also calculates clad surface heat flux, DNB heat flux, and DNB ratio, and many other parameters.

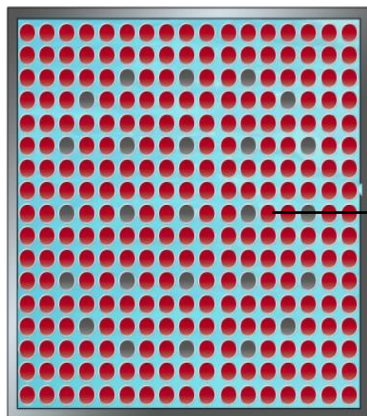


Fig. 2 Fuel assembly

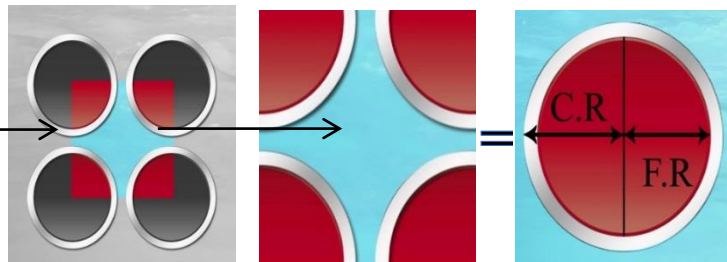


Fig. 3 coolant sub-channels

## **2. Previous study [3]**

A neutronic analysis of the AP-1000 reactor core has been done using LEOPARD, 2DB, and TLINX codes in a previous study, which has been published at the 15th Arab atomic energy conference in Aswan, 2021. The neutronic parameters such as power distribution that have been obtained in previous study are used in this study.

## **3. Methodology**

To determine the hot channels, the hottest assembly has been described in the **2DB** code, which includes 264 fuel rods and 25 control rods. The control rods are assumed to be withdrawn and their regions are full of water. By running **2DB** input files, the power distribution on the assembly is found, and it is noted that the channels in the corner have the highest power produced (139.0267 KW), as shown in figure (4.13). The hot channel factor (FR) (The ratio of power generation in a hot channel to that in an average channel) can be calculated.

$$FR = \frac{\text{power generation in the hot channel}}{\text{power generation in an average channel}}$$

Where power generation in an average channel =  $\frac{\text{thermal Power generated in entire core}}{\text{number of fuel rods in the core}}$

$$\text{Power generation in an average channel} = \frac{3400}{41448} = 0.08203 \text{ MW} = 82.3049 \text{ KW}$$

$$\text{FR} = \frac{139.027}{82.03049} = 1.69$$

0.00	0.00	0.00	0.00	0.00	0.00	0.00	0.00	0.00	0.00
123.24	123.17	123.39	123.91	124.26	125.04	127.05	131.22	139.07	0.00
117.53	116.47	116.76	118.37	117.70	117.70	119.06	122.88	131.22	0.00
0.00	114.13	114.54	0.00	116.56	116.53	116.35	119.07	127.05	0.00
111.91	110.77	111.27	113.67	115.15	0.00	116.53	117.71	125.06	0.00
110.64	109.52	109.99	112.25	112.89	115.16	116.58	117.73	124.28	0.00
0.00	110.01	110.40	0.00	112.27	113.69	0.00	118.41	123.94	0.00
109.45	108.29	108.60	110.41	110.01	111.30	114.58	116.81	123.45	0.00
109.21	108.04	108.30	110.04	109.56	110.82	114.20	116.55	123.25	0.00
0.00	109.21	109.47	0.00	110.69	111.97	0.00	117.62	123.33	0.00

Fig. 4 Power distribution (KW) in a quarter of the hottest assembly

#### 4. Results:

##### 4.1. Average channel

From the neutronic parameters that were obtained in the previous study, a thermal hydraulic analysis was simulated using the **MITH** code depending on **FR** value and the data on a table (1), choosing the number of discrete intervals as 40 meshes for drawing and 100 meshes for studying (for best accuracy).

The **MITH** output file has results that are shown in Tables (2) and (3).

Table (1) AP1000 specifications <sup>[1]</sup>.

Channel length (Z)	Heat flux Btu/hr-ft <sup>2</sup>	T-fluid °C	T-clad °C	T-fuel surface °C	Temp. fuel center °C	Fluid density (Lbs/ft <sup>3</sup> )	Fluid enthalpy Btu/lbm-°F
1	2.53E+04	265.29	267.76	281.58	345.72	47.8	528.93
2	5.05E+04	265.51	270.43	297.98	425.86	47.78	529.4
3	7.54E+04	265.87	273.21	314.32	505.16	47.74	530.18
4	9.97E+04	266.37	276.08	330.49	583.12	47.69	531.27
5	1.24E+05	267.00	279.02	346.41	659.25	47.62	532.66
6	1.47E+05	267.77	282.01	361.96	733.09	47.53	534.34
7	1.69E+05	268.66	285.04	377.04	804.18	47.43	536.31
8	1.90E+05	269.67	288.07	391.58	872.08	47.32	538.54
9	2.10E+05	270.79	291.10	405.46	936.38	47.2	541.02
10	2.28E+05	272.01	294.01	418.52	996.58	47.06	543.75
11	2.45E+05	273.32	297.71	431.61	1053.23	46.91	546.7
12	2.61E+05	274.82	299.48	441.94	1103.31	46.73	549.85
13	2.75E+05	276.23	302.42	452.56	1149.59	46.57	553.19
14	2.88E+05	277.72	305.14	462.04	1190.44	46.39	556.69
15	2.98E+05	279.29	307.76	470.44	1225.71	46.2	560.34
16	3.07E+05	280.91	310.25	477.72	1255.21	46	564.1
17	3.14E+05	282.57	312.58	483.81	1278.72	45.8	567.97
18	3.19E+05	284.26	314.75	488.67	1296.10	45.58	571.9
19	3.22E+05	285.97	316.73	492.28	1307.25	45.36	575.89
20	3.23E+05	287.68	318.51	494.60	1312.09	45.14	579.9
21	3.22E+05	289.38	320.08	495.62	1310.60	44.91	583.91
22	3.19E+05	291.07	321.42	495.34	1302.78	44.69	587.9
23	3.14E+05	292.71	322.54	493.77	1288.68	44.46	591.84
24	3.07E+05	294.32	323.43	490.90	1268.38	44.23	595.7
25	2.98E+05	295.87	324.07	486.76	1242.03	44.01	599.47
26	2.88E+05	297.35	324.48	481.38	1209.78	43.79	603.11
27	2.75E+05	298.76	324.66	474.80	1171.83	43.58	606.62
28	2.61E+05	300.09	324.61	467.07	1128.44	43.38	609.96
29	2.45E+05	301.33	324.24	458.14	1079.77	43.19	613.11
30	2.28E+05	302.47	323.83	448.34	1026.40	43.01	616.06
31	2.10E+05	303.53	323.09	437.46	968.38	42.84	618.78
32	1.90E+05	304.49	322.15	425.66	906.17	42.69	621.27
33	1.69E+05	305.34	321.02	413.02	840.17	42.55	623.5
34	1.47E+05	306.08	319.69	399.63	770.77	42.43	625.46
35	1.24E+05	306.71	318.17	385.56	698.40	42.32	627.14
36	9.97E+04	307.23	316.48	370.89	623.52	42.23	628.53
37	7.54E+04	307.64	314.62	355.73	546.57	42.16	629.62

<b>38</b>	5.05E+04	307.93	312.61	340.16	468.04	42.11	630.4
<b>39</b>	2.53E+04	308.11	310.45	324.27	388.41	42.08	630.87
<b>40</b>	4.73E-01	308.17	308.17	308.17	308.17	42.07	631.03

Table (2) Average temperatures, heat flux, fluid density & enthalpy

Parameter	AP-1000	
	English units	SIU
Thermal Hydraulic Specifications		
Reactor core Thermal Power (MWt)	3400	3400
System pressure, nominal	2250 psia	15.513 MPa
Total flow rate	113.5 X10 <sup>6</sup> lbm/hr	51.48X10 <sup>6</sup> Kg/hr
Fuel weight, as uranium dioxide	211,588 lb	95974.70 kg
Fuel Design		
Type of fuel assemblies	17X17	
Number of fuel assemblies	157	
Uranium dioxide rods per assembly	264	
Number of all Fuel Rods	41,448	
Engineering Specifications		
Fuel element outside diameter	0.374 in	0.945 cm
Clad thickness	0.0225 in	0.05715 cm
Core diameter, equivalent	119.7 in	3.0438 m
Core height	14 ft	4.267 m
The active core volume	1093.74 ft <sup>3</sup>	30.971318 m <sup>3</sup>
Assembly pitch	8.46456 in	21.5 cm
Rod pitch	0.496 in	1.2598 cm
Enrichments		
Fuel Enrichment First Cycle	Region 1	2.35
	Region 2	3.40
	Region 3	4.45

Table (3) Thermal hydraulic average parameter

Parameter	SIU	British unit
Average coolant density	721.38 Kg/m <sup>3</sup>	45.034 Lbs/Ft <sup>3</sup>
Core pressure drop	81 Pa	11.7490 Psi

Fig. (5) Represents the variation of heat flux versus channel length.

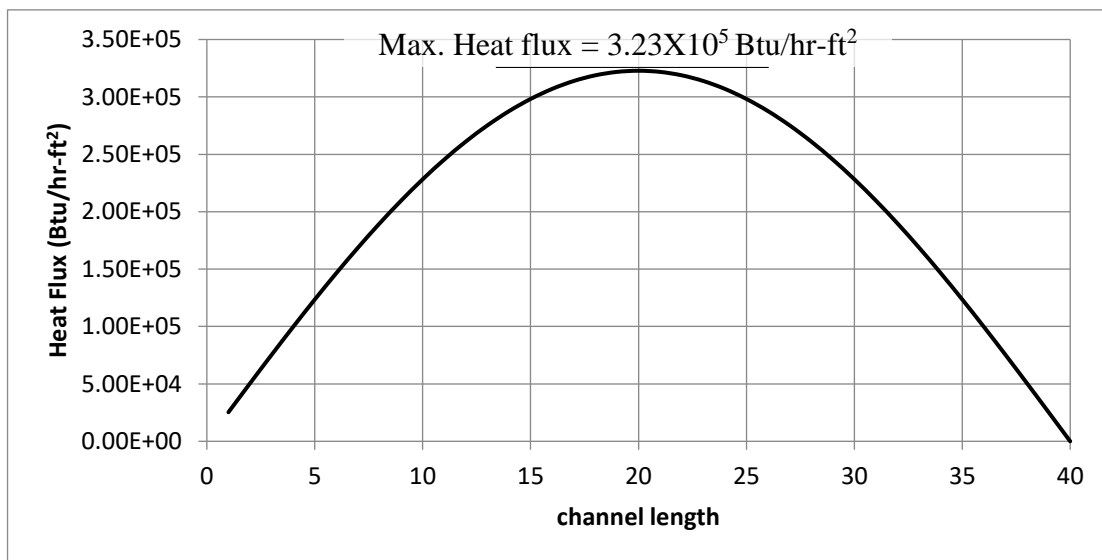
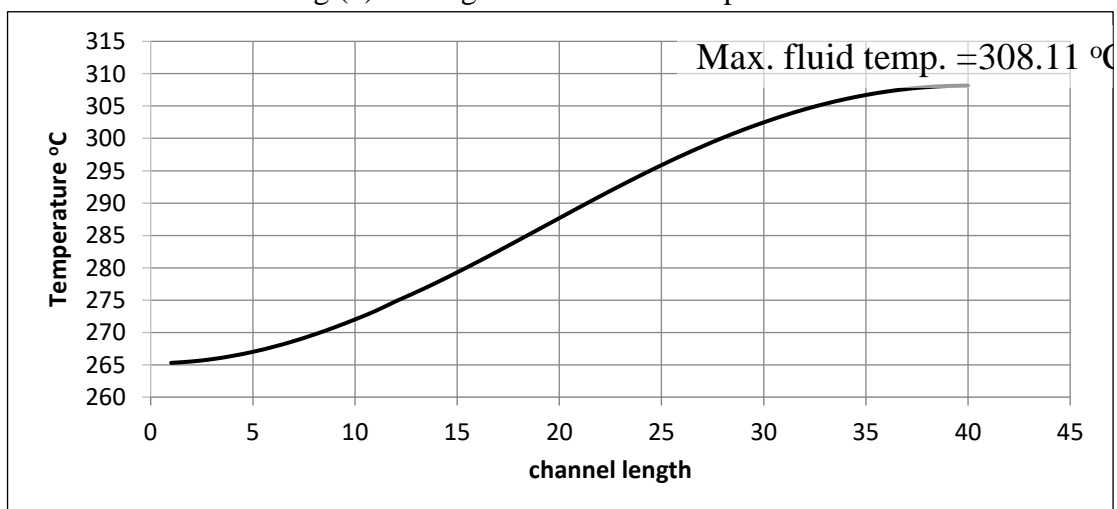


Fig (5) Average channel heat flux.

**Figure 5 shows that the heat flux increases with a channel length (from bottom to top), with a maximum value of ( $3.23 \times 10^5$  Btu/hr-ft<sup>2</sup>) at the center of the channel length ( $\approx 2.14$  m), then it begins to decrease using the (sin) formula until it equals ( $4.73 \times 10^1$ ) at the end of the channel length ( $\approx 4.267$  m). Fig. (4.15) represents the variation of coolant temperature with channel length. Fig. (6) represents the variation of coolant temperature with channel length.**

Fig (6) Average channel fluid temperature.



It can be noted from figure 6 that the coolant temperature increases versus channel length (Z) due to heat transfer from fuel through cladding to fluid (H<sub>2</sub>O). As channel

length increases, the quantity of heat transferred ( $Q = h.A.(T_1 - T_2)$ ) decreases due to the difference in  $T_2$  values at the bottom and in the center of channel length.

Fig. (7) represents the variation of clad temperature versus channel length.

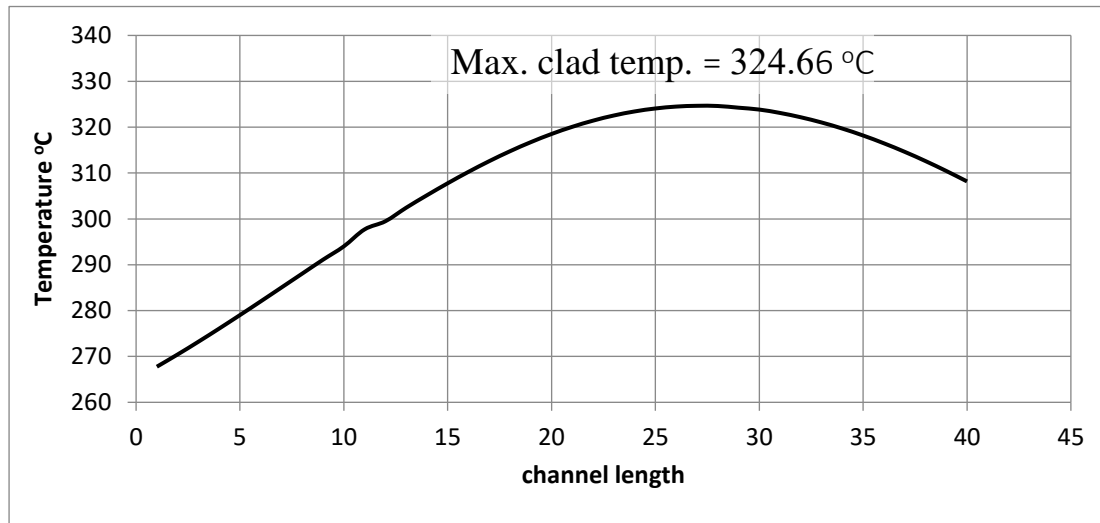


Fig (7) Average channel clad temperature.

In the case of clad, the temperature rises as channel length increase until it reaches mesh # 27 (2.88 m) and reaches the maximum value of (324.65 °C), then falls as channel length increases until it reaches (308.17°C) at the top end of the channel length at 4.267 m.

Fig. (8) represents the variation of center and surface fuel temperatures versus channel length.

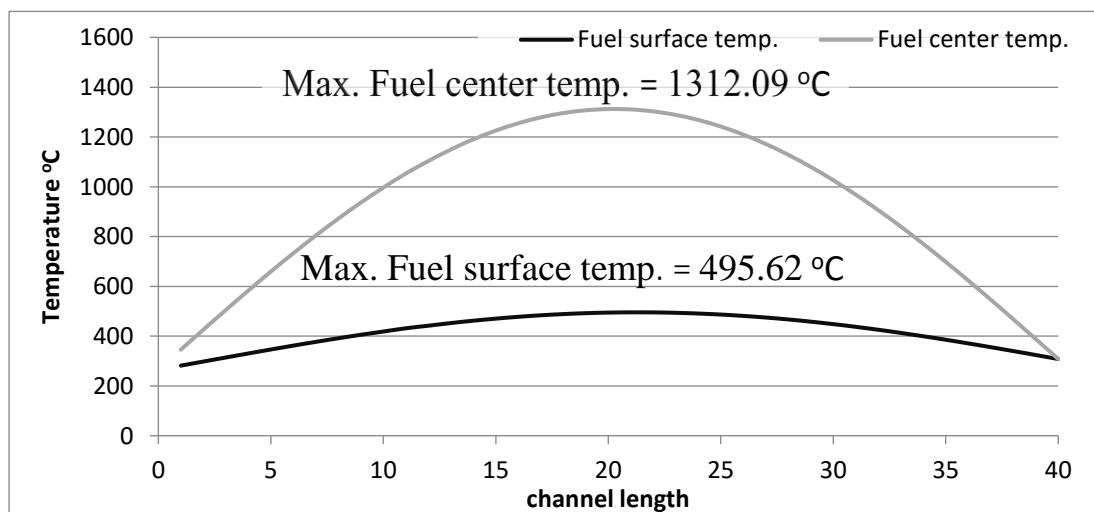


Fig (8) Average channel fuel temperatures.

From the figure, it can be noted that:

- 1- The maximum fuel surface temperature is 495.62 °C at mesh # 21 ( $\approx 2.24$ m).
- 2- The maximum fuel center temperature is about 1312 °C.

To find the position of the maximum center fuel temperature exactly, 100 meshes are used in the **MITH** code, and it is found that it occurs at mesh # 51 nearly, 21.76 m.

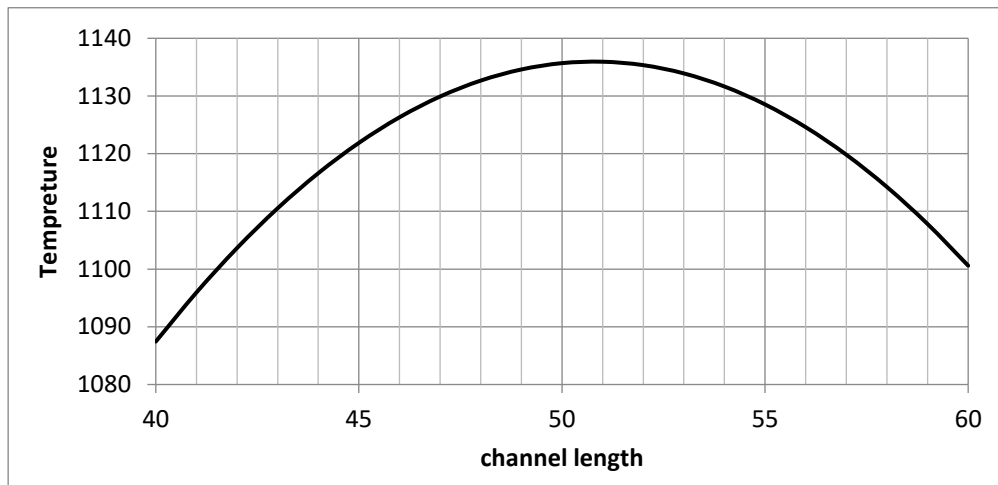


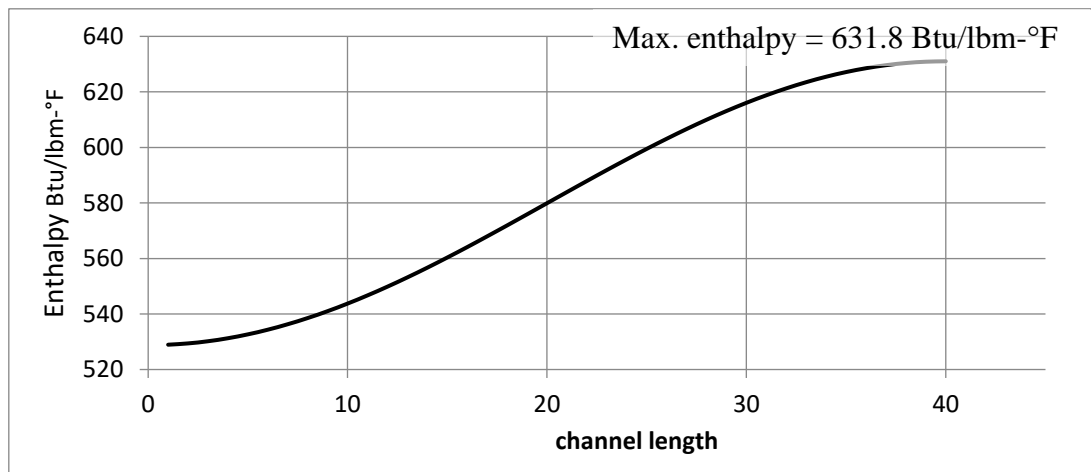
Fig. (9) Center of fuel temperature vs. channel length using 100 meshes.

Table (4) the maximum center fuel temperature

Mesh #	Temperature °F	Temperature °C
50	2101.85	1135.694
51	2102.29	1135.939
52	2101.23	1135.35

Fig.

(10)



represents the enthalpy temperature versus channel length.

Fig. (10) Average channel enthalpy.

As shown in Fig. (10), as the fluid temperature rises versus channel length, the value of enthalpy increases until it gets to the maximum value (631 Btu/lbm-°F) at the end of channel length.

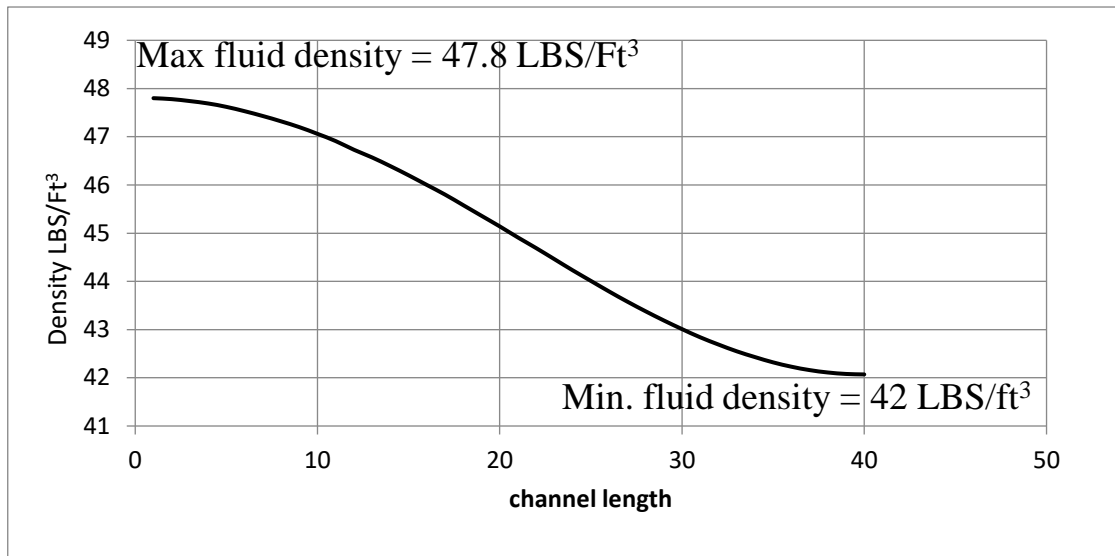


Fig. (11) Average channel fluid density.

The last figure shows the decrease in fluid density versus channel length due to an increase in fluid temperature where the density of fluid is equal to 42 LBS/Ft³ at the end channel length.

#### **4.2.Hot channels**

The **MITH** output file includes also hot channel parameters as shown in Table (5) and the figures below.

Channel length (Z)	Heat flux Btu/hr-ft <sup>2</sup>	T-fluid °C	T-clad °C	T-fuel surface °C	T-fuel center °C	Enthalpy Btu/lbm °F	DNB Heat Flux Btu/hr-ft <sup>2</sup>	<i>DNBR</i> <i>DNB/Heat-flux</i>
0	0	265.22	265.22	265.22	265.22	528.77	2.10E+06	*****
1	4.28E+04	265.34	269.52	292.87	401.26	529.04	2.10E+06	4.91E+01
2	8.53E+04	265.71	274.03	320.58	536.71	529.84	2.09E+06	2.45E+01
3	1.27E+05	266.32	278.72	348.19	670.71	531.16	2.08E+06	1.63E+01
4	1.69E+05	267.16	283.56	375.52	802.44	533	2.06E+06	1.22E+01
5	2.09E+05	268.22	288.51	402.39	931.09	535.35	2.04E+06	9.78E+00
6	2.48E+05	269.51	293.54	428.64	1055.86	538.19	2.02E+06	8.14E+00
7	2.85E+05	271.01	298.62	454.11	1175.97	541.51	1.99E+06	6.97E+00
8	3.21E+05	272.70	304.79	479.71	1291.77	545.27	1.95E+06	6.09E+00
9	3.54E+05	274.74	308.18	501.46	1398.71	549.47	1.91E+06	5.40E+00
10	3.86E+05	276.68	313.41	523.84	1500.76	554.08	1.87E+06	4.86E+00
11	4.15E+05	278.81	318.40	544.69	1595.24	559.06	1.83E+06	4.41E+00
12	4.41E+05	281.10	323.28	564.04	1681.74	564.39	1.78E+06	4.04E+00
13	4.65E+05	283.53	328.01	581.74	1759.72	570.03	1.73E+06	3.73E+00
14	4.86E+05	286.07	332.52	597.68	1828.66	575.95	1.68E+06	3.47E+00
15	5.04E+05	288.69	332.86	607.79	1884.19	582.11	1.63E+06	3.24E+00
16	5.19E+05	291.38	332.87	615.90	1929.84	588.48	1.58E+06	3.04E+00
17	5.30E+05	294.12	332.88	622.24	1965.64	595.01	1.52E+06	2.87E+00
18	5.39E+05	296.86	332.88	626.81	1991.37	601.66	1.47E+06	2.73E+00
19	5.44E+05	299.58	332.88	629.55	2006.86	608.4	1.41E+06	2.60E+00
20	5.45E+05	302.27	332.87	630.46	2012.03	615.18	1.36E+06	2.49E+00
21	5.44E+05	304.87	332.86	629.53	2006.84	621.96	1.31E+06	2.40E+00
22	5.39E+05	307.43	332.84	626.77	1991.33	628.7	1.25E+06	2.33E+00
23	5.30E+05	309.91	332.83	622.20	1965.59	635.35	1.20E+06	2.27E+00
24	5.19E+05	312.30	332.81	615.83	1929.78	641.88	1.15E+06	2.22E+00
25	5.04E+05	314.59	332.79	607.73	1884.13	648.25	1.10E+06	2.19E+00
26	4.86E+05	316.75	332.75	597.91	1828.89	654.41	1.06E+06	2.17E+00
27	4.65E+05	318.78	332.72	586.46	1764.43	660.33	1.01E+06	2.18E+00
28	4.41E+05	320.64	332.68	573.43	1691.14	665.97	9.70E+05	2.20E+00
29	4.15E+05	322.37	332.64	558.93	1609.48	671.3	9.31E+05	2.25E+00
30	3.86E+05	323.93	332.58	543.02	1519.93	676.28	8.95E+05	2.32E+00
31	3.54E+05	325.33	332.53	525.81	1423.06	680.89	8.62E+05	2.43E+00
32	3.21E+05	326.58	332.47	507.39	1319.46	685.09	8.32E+05	2.59E+00
33	2.85E+05	327.67	332.40	487.89	1209.76	688.86	8.05E+05	2.82E+00
34	2.48E+05	328.59	332.32	467.42	1094.64	692.17	7.81E+05	3.15E+00
35	2.09E+05	329.37	332.23	446.11	974.82	695.01	7.61E+05	3.65E+00
36	1.69E+05	330.00	332.12	424.08	851.01	697.36	7.45E+05	4.42E+00

<b>37</b>	1.27E+05	330.33	331.99	401.46	723.98	699.2	7.32E+05	5.75E+00
<b>38</b>	8.53E+04	330.32	331.82	378.38	594.50	700.53	7.22E+05	8.47E+00
<b>39</b>	4.28E+04	330.31	331.57	354.92	463.32	701.33	7.17E+05	1.67E+01
<b>40</b>	7.99E-01	<b>330.30</b>	<b>330.30</b>	<b>330.30</b>	<b>330.30</b>	<b>701.59</b>	7.15E+05	8.94E+05

Table (5) Hot channels temperatures heat flux & DNB flux

The hot channel fuel temperature versus channel length is shown in fig. (12)

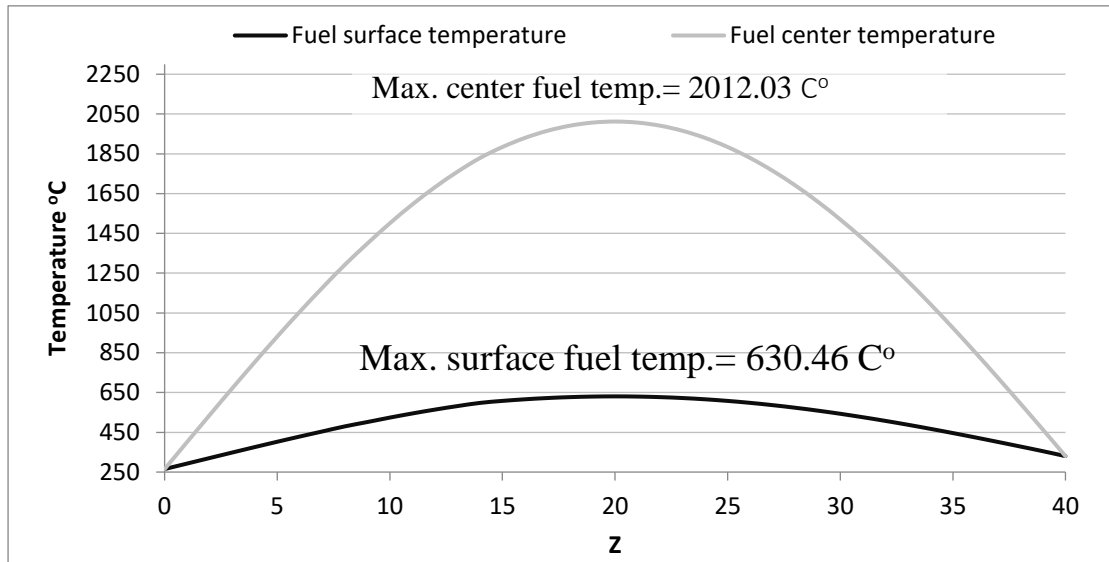


Fig. (12) Hot channel fuel temperature.

It can be noted from the figure that:

- 1- The maximum temperature of the fuel surface in the hot channel is 630.46 °C
- 2- The maximum center fuel temperature in the hot channel is 2012.03 °C which is still within the safety limit.

Fig (13) represents the variation of hot channel fluid temperature.

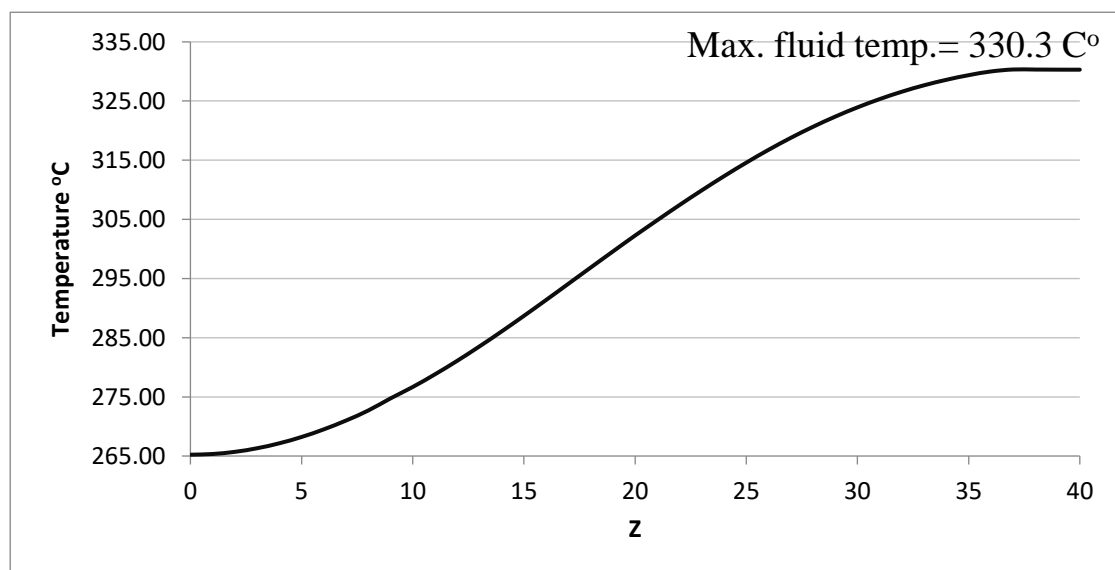


Fig. (13) Hot channel fluid temperature.

As shown in Fig. (13), fluid temperature increases versus channel length (Z) due to heat transfer from fuel through clad to fluid.

Fig. (14) Shows the critical heat flux and average heat flux curve versus channel length (Z). The minimum distance between these two curves represents the DNBR, where the reactor core must be designed to keep the DNBR larger than the minimum allowable value (1.25 for AP1000 at least) [1]. As shown in fig. (4.23), the minimum DNBR is 2.17 which means the reactor is working within the safe limit.

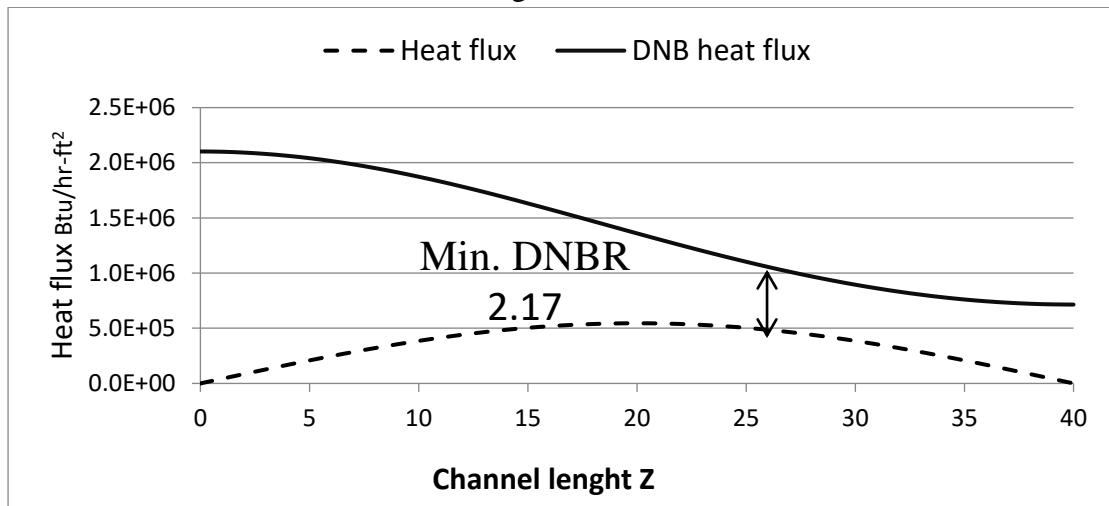
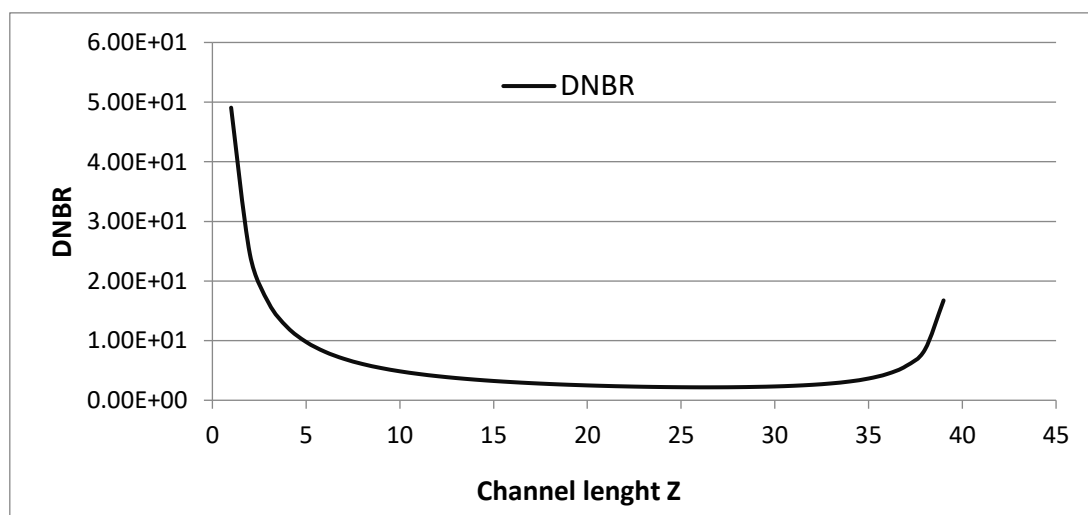


Fig. (14) Hot channel heat flux vs. channel length (Z)

Fig. (15) Represents the variation of DNBR with. Channel length.

Where  $DNBR = \frac{q''_{DNB}(Z)}{q''(Z)}$

Fig. (15) DNBR vs. channel length (Z)



## Conclusion

- The code used in the current study showed a good ability to deal with modern nuclear reactors. The results obtained were well consistent with what was expected.
- The fuel elements' temperatures were as it was expected, while the minimum DNBR within the limited values for PWR.

**Recommendations for future work:**

Do a thermal-hydraulic analysis for AP1000 poisoned core (with burnable poison and soluble boron) and compare the results with this study, the fuel element temperatures for the hottest channel should decrease as well as DNBR.

**References:**

- [1]. AP1000 Design Control Document Tier 2 Material Revision 16 section 4.3-46
- [2]. LAEE report - nuclear power to produce electricity globally and its prospects in Libya -4.8 Nuclear reactors suitable for Libya 2013, pp 67.
- [3]. Tariq Zakariya Malatim, Amal S. Dakhil, Benchmarking of using LEOPARD /2DB codes for neutronic calculation of the Westinghouse AP1000, Arab atomic energy conference, 2021
- [4]. Gangloff, W. Westinghouse AP600 Advanced Nuclear Plant Design (PDF) (Technical report). IAEA
- [5]. Westinghouse, 2011. AP1000 Design Control Document Rev. 19. Section 4.3 – Reactor, Nuclear Design.
- [6]. Bahman Zohuri, Nima Fathi, Thermal-Hydraulic Analysis of Nuclear Reactors, 2015.
- [7]. Nikolay I. Kolev, Multiphase Flow Dynamics 4 - Nuclear Thermal Hydraulics -1<sup>st</sup> Edition, 2006, pp 156.